Journal of Sound and Vibration 392 (2017) 232–239

Contents lists available at ScienceDirect

Journal of Sound and Vibration

journal homepage: www.elsevier.com/locate/jsvi

The dynamics of large-scale arrays of coupled resonators

Chaitanya Borra [a], Conor S. Pyles [b], Blake A. Wetherton [b], D. Dane Quinn [a,*], Jeffrey F. Rhoads [b]

[a] Department of Mechanical Engineering, The University of Akron, Akron, OH 44325, USA
[b] School of Mechanical Engineering, Birck Nanotechnology Center, and Ray W. Herrick Laboratories, Purdue University, West Lafayette, IN 47907

ARTICLE INFO

Article history:
Received 29 June 2016
Received in revised form
11 December 2016
Accepted 12 December 2016
Available online 20 December 2016

Keywords:
Microelectromechanical systems
Globally-coupled resonators
Nonlinear dynamical systems
Integro-differential equations

ABSTRACT

This work describes an analytical framework suitable for the analysis of large-scale arrays of coupled resonators, including those which feature amplitude and phase dynamics, inherent element-level parameter variation, nonlinearity, and/or noise. In particular, this analysis allows for the consideration of coupled systems in which the number of individual resonators is large, extending as far as the continuum limit corresponding to an infinite number of resonators. Moreover, this framework permits analytical predictions for the amplitude and phase dynamics of such systems. The utility of this analytical methodology is explored through the analysis of a system of N non-identical resonators with global coupling, including both reactive and dissipative components, physically motivated by an electromagnetically-transduced microresonator array. In addition to the amplitude and phase dynamics, the behavior of the system as the number of resonators varies is investigated and the convergence of the discrete system to the infinite-N limit is characterized.

1. Introduction

Coupled dynamical systems have garnered increasing interest over the past three decades due to their ability to describe the complex behaviors attendant to fields such as mathematical biology (see, for example [1,2]) and their ability to describe collective and emergent behavior in physics and engineering contexts. For example, coupled ensembles of oscillators or resonators have been used in the modeling, analysis, design, and characterization of fiber lasers, oil pipelines, bladed disk assemblies, and antennas, amongst other pertinent systems (see, for example, [3–6]). One area of engineering research that has recently advanced the understanding of coupled dynamical systems is that related to micro- and nanoelectromechanical systems, or so-called MEMS and NEMS (see, for example, [7–21]). In this area of application there exist natural economies of scale, which allow for very large degree-of-freedom ensembles, accompanied by noise and parametric uncertainty. The emergent dynamics of such systems are often avoided, yet with proper system design, the global dynamics can be exploited to provide system performance that cannot be realized with individual components. Accordingly, these systems offer a certain appeal for the traditional analyst, as well as the practitioner who values the utility of collective and emergent behaviors in applications as broad as mass sensing, signal processing, pattern generation, and even neural computing.

* Corresponding author.
E-mail addresses: cb143@zips.uakron.edu (C. Borra), pyles@purdue.edu (C.S. Pyles), bwethert@purdue.edu (B.A. Wetherton), quinn@uakron.edu (D.D. Quinn), jfrhoads@purdue.edu (J.F. Rhoads).

http://dx.doi.org/10.1016/j.jsv.2016.12.021
0022-460X/

Despite the rapid growth in interest related to coupled dynamical systems, analytical advancements in this area have been comparatively slow. Today, most analytical methods are based on mathematical reductions to phase-only models or leverage system symmetries to predict and explain observed dynamical behaviors. Unfortunately, these methods are ill-suited for many practical problems, which feature *both amplitude and phase* dynamics, inherent element-level parameter variation (mistuning), nonlinearity, and/or noise.

This work seeks to help fill this apparent analytical gap through the presentation of a systematic analytical approach which is amenable to the aforementioned problems and is adapted from prior work by [22]. This analytical framework utilizes: (i) a discrete-to-continuous system transformation, followed by (ii) the application of a perturbation method on the continuum representation and (iii) the use of an iterative numerical method to solve the resulting integral equations, and, finally, (iv) interpretation of the results acquired from the continuous analog or, following an additional transformation, the discrete representation.

The aforementioned framework is explored through an investigation of the dynamics of a specific system of interest: a globally coupled microresonator array with reactive and/or dissipative coupling, together with element-level dynamics that contain weak stiffness nonlinearities. To this end, this work presents not only a new analytical framework suitable for the analysis of large degree-of-freedom, coupled dynamical systems, but also provides an analytical pathway suitable for the design and development of coupled micro- and nanoresonator arrays, facilitating their use in very-large-system-integration (VLSI)-like contexts.

2. A discrete system of coupled resonators

Equations of motion

The coupled dynamical system of interest herein is the electromagnetically-transduced microresonator array that was explored, both analytically and experimentally, by the authors in prior work ([23,12]). This microsystem is actuated by Lorentz forces resulting from interactions between current-carrying conducting metal loops deposited on the resonator's surface and an external magnetic field ([24,25]). Likewise, the system exploits the back electromotive force (EMF) resulting from the conductor passing through the magnetic field for sensing. In this system, global dissipative coupling arises naturally due to the current that identically flows through each individual resonator and the resulting electromagnetic interactions described previously. For this work, this coupling is augmented by a global reactive coupling component for the sake of generality. These coupling terms are in contrast to nearest neighbor coupling that might arise from, for example, localized mechanical interactions ([6]). Accordingly, the differential equations of motion that govern the coupled system's dynamics, assuming finite but not large displacements (i.e. tip deflections approximately one order of magnitude smaller than the beam length), are given by

$$m_i\ddot{z}_i + c_i\dot{z}_i + k_i z_i + \gamma_i z_i^3 - \frac{\alpha}{N}\sum_{j=1}^{N}\dot{z}_j - \frac{\beta}{N}\sum_{j=1}^{N} z_j = f_i(t). \tag{1}$$

Here, each individual resonator in the N-element array is characterized by the index i and has an associated displacement z_i. Likewise, m_i, c_i, and k_i represent the mass, damping, and stiffness of each resonator, while γ_i parameterizes the strength of the nonlinearity. The parameters α and β characterize the overall strength of the dissipative and reactive global respectively. Finally, each resonator is subject to an external time-dependent excitation represented by $f_i(t)$.

3. Continuum model

3.1. Formulation

The discrete system of coupled resonators can be recast in a continuum formulation, allowing for a compact description of the resulting dynamics, similar to the system of coupled oscillators considered by [22]. In particular, the global dissipative and reactive coupling terms can be expressed as integrals over the population of resonators. As an example, the dissipative coupling term in Eq. (1) can be written as

$$\frac{\alpha}{N}\sum_{j=1}^{N}\dot{z}_j = \frac{\alpha}{N}\int_{-\infty}^{\infty}\left(\dot{z}(t;\, n)\sum_{j=1}^{N}\delta(n - s_j)\right)\mathrm{d}n, \quad \text{with} \quad \dot{z}_j \equiv \dot{z}(t;\, s_j), \tag{2}$$

where $\delta(x)$ is a Dirac delta function and the distribution parameter s_j identifies the j^{th} resonator. As a result, the discrete system of coupled resonators can be written as a single integro-differential equation of the form

$$m_s\ddot{z}(t;\, s) + \epsilon c_s\dot{z}(t;\, s) + k_s z(t;\, s) + \epsilon\gamma_s z^3(t;\, s) \quad - \epsilon\alpha\int_{-\infty}^{\infty}\dot{z}(t;\, n)\rho_N(n)\mathrm{d}n - \epsilon\beta\int_{-\infty}^{\infty} z(t;\, n)\rho_N(n)\mathrm{d}n = \epsilon f_s(t), \tag{3}$$

where a population density function $\rho_N(s)$ can be identified as

$$\rho_N(s) \equiv \frac{1}{N}\sum_{j=1}^{N}\delta(s - s_j). \tag{4}$$

Again, the variable s_i identifies an individual resonator so that $m_i \equiv m_{s_i}$ and so forth. Note that the scaling parameter ϵ has been introduced so that the resonator damping, nonlinearity, and coupling terms are assumed to be small. Finally, the amplitude of the external forcing is assumed to be same order as the damping, scaled by ϵ. With this, the dominant response of the system is $O(1)$ for those resonators tuned to the excitation frequency Ω. The external forcing is further assumed to be harmonic with frequency Ω and identical for each resonator, so that

$$\epsilon f_s(t) = \epsilon F_0 \sin(\Omega t). \tag{5}$$

This formulation can likewise be extended to a continuum distributions of resonators through a general population density function $\rho(s)$, assumed to satisfy

$$\int_{-\infty}^{\infty}\rho(n)\mathrm{d}n = 1. \tag{6}$$

For example, if the population mass follows a continuous normal distribution with mean m_0 and standard deviation σ, then

$$\rho(s) = \frac{e^{-\left(\frac{s-m_0}{\sqrt{2}\sigma}\right)^2}}{\sigma\sqrt{2\pi}}. \tag{7}$$

Here, we consider a population of resonators such that

$$m_s = m_0 + \epsilon s, \quad c_s = c, \quad k_s = k, \quad \gamma_s = \gamma. \tag{8}$$

Thus, the distribution parameter s is identified with the detuning of resonator mass from the mean value m_0 of the population. Note that the damping and stiffness parameters (c, k, γ) are identical for each resonator. With these, Eq. (3) reduces to

$$(m_0 + \epsilon s)\ddot{z}(t; s) + \epsilon c\dot{z}(t; s) + kz(t; s) + \epsilon\gamma z^3(t; s) \quad - \epsilon\alpha\int_{-\infty}^{\infty}\dot{z}(t; n)\rho(n)\mathrm{d}n - \epsilon\beta\int_{-\infty}^{\infty}z(t; n)\rho(n)\mathrm{d}n = \epsilon F_0\sin(\Omega t). \tag{9}$$

Finally, the system is assumed to be tuned such that

$$\frac{k}{m_0} = \Omega^2. \tag{10}$$

3.2. Perturbation solution

We note that in Eq. (9) the distribution parameter s identifies a particular resonator, but the dynamics of each resonator can be described by a single-degree-of-freedom, Duffing-like model, subject to the time-varying global coupling functions parameterized by α and β. Therefore, a standard perturbation approach is applied to each resonator in Eq. (9), so that

$$z(t; s) = z_0(t; s) + \epsilon z_1(t; s) + O(\epsilon^2). \tag{11}$$

Expanding in ϵ and collecting the coefficients of ϵ^i in the resulting equation, yields

$$O(\epsilon^0)\text{: } \ddot{z}_0 + \Omega^2 z_0 = 0, \tag{12a}$$

$$O(\epsilon^1)\text{: } \ddot{z}_1 + \Omega^2 z_1 = \frac{F_0}{m_0}\sin(\Omega t) - \left(s\ddot{z}_0 + c\dot{z}_0 + \gamma z_0^3\right) \quad + \frac{\alpha}{m_0}\int_{-\infty}^{\infty}\dot{z}_0(t; n)\rho(n)\mathrm{d}n + \frac{\beta}{m_0}\int_{-\infty}^{\infty}z_0(t; n)\rho(n)\mathrm{d}n. \tag{12b}$$

To lowest order, the response of $z_0(t; s)$ is

$$z_0(t; s) = A(s)\sin(\Omega t) + B(s)\cos(\Omega t), \tag{13}$$

where $A(s)$ and $B(s)$ are unspecified. Introducing this solution into the next order of the approximation leads to secular terms that must be removed for a uniformly-valid solution. Specifically, the unspecified coefficients must satisfy

$$\frac{F_0}{m_0} + s\Omega^2 A(s) + c\Omega B(s) - \frac{3\gamma}{4}A(s)\left[A^2(s) + B^2(s)\right] \quad = \frac{\alpha}{m_0}\Omega\int_{-\infty}^{\infty}B(n)\rho(n)\mathrm{d}n - \frac{\beta}{m_0}\int_{-\infty}^{\infty}A(n)\rho(n)\mathrm{d}n, \tag{14a}$$

$$s\Omega^2 B(s) - c\Omega A(s) - \frac{3\gamma}{4}B(s)\left[A^2(s) + B^2(s)\right] \quad = -\frac{\alpha}{m_0}\Omega\int_{-\infty}^{\infty}A(n)\rho(n)\mathrm{d}n - \frac{\beta}{m_0}\int_{-\infty}^{\infty}B(n)\rho(n)\mathrm{d}n. \tag{14b}$$

These nonlinear integral equations can be solved for $A(s)$ and $B(s)$ to provide the $O(\epsilon^0)$ approximation for the response of

the population in the presence of global dissipative and reactive coupling. It is worth noting that in these equations the integral terms are definite, so that they are independent of s, although they most certainly depend on the unknown functions $[A(s), B(s)]$. Finally, the amplitude and phase response functions can be subsequently expressed as

$$\begin{aligned} &X(s) = \sqrt{A^2(s) + B^2(s)}, \\ &\tan\Phi(s) = \frac{B(s)}{A(s)}, \end{aligned} \qquad \longrightarrow \quad z_0(t; s) = X(s)\sin\big[\Omega t + \Phi(s)\big], \tag{15}$$

such that $A(s) = X(s)\cos\Phi(s)$ and $B(s) = X(s)\sin\Phi(s)$.

3.3. Iterative solution

The aforementioned integral equations can be solved by identifying the integral terms as

$$V \equiv \int_{-\infty}^{\infty} A(n)\rho(n)\mathrm{d}n, \quad W \equiv \int_{-\infty}^{\infty} B(n)\rho(n)\mathrm{d}n, \tag{16}$$

such that the resulting equations can be written as

$$\frac{F_0}{m_0} + s\Omega^2 A(s) + c\Omega B(s) - \frac{3\gamma}{4}A(s)\big[A^2(s) + B^2(s)\big] = \frac{\alpha}{m_0}\Omega W - \frac{\beta}{m_0}V, \tag{17a}$$

$$s\Omega^2 B(s) - c\Omega A(s) - \frac{3\gamma}{4}B(s)\big[A^2(s) + B^2(s)\big] = -\frac{\alpha}{m_0}\Omega V - \frac{\beta}{m_0}W. \tag{17b}$$

These algebraic equations can be then solved for $[A(s), B(s)]$. Note that these functions must be consistent with the definitions of V and W given above, so that Eq. (16) define a self-consistency condition for the functions $A(s)$ and $B(s)$. We refer to V and W as the global self-consistency constants.

For $\gamma \neq 0$ the nonlinear algebraic system given in Eq. (17b) cannot be solved in closed form, thus the self-consistency conditions given in Eq. (16) cannot be evaluated in closed form to solve for $A(s)$ and $B(s)$. Instead, a numerical method is used to determine the functions $A(s; V_i, W_i)$ and $B(s; V_i, W_i)$ for specified values of $(V = V_i, W = W_i)$ in Eqs. (17b). The associated squared error in the solution is given as

$$\mathcal{E} = \left[V_i - \int_{-\infty}^{\infty} A(n; V_i, W_i)\rho(n)\mathrm{d}n,\right]^2 + \left[W_i - \int_{-\infty}^{\infty} B(n; V_i, W_i)\rho(n)\mathrm{d}n,\right]^2. \tag{18}$$

Finally, an optimization strategy is employed to minimize $\mathcal{E}$, thus converging on the solution. This approach is implemented in MATLAB using the functions `fsolve` to determine $A(s; V_i, W_i)$ and $B(s; V_i, W_i)$, with `fmincon` employed to minimize the resulting error.

Note that the response of any individual resonator is influenced by the population only through the values of V and W. Thus, these terms characterize the influence of the global coupling within the system. In fact, the response functions $A(s)$ and $B(s)$ can be solved for any value of s, while only those resonators that influence the population density $\rho(s)$ contribute to the global self-consistency constants V and W.

4. Results and discussion

The analytical predictions for the stationary solutions can be compared against results obtained from direct numerical simulation of the discrete equations of motion. Unless noted, here we choose $\epsilon = 10^{-2}$; the remaining default parameters for the system are

$$m_0 = 1, \quad \Omega = 1, \quad c = 0.50, \quad F = 1, \quad \alpha = 2.00, \quad \beta = 5.00. \tag{19}$$

With $\gamma = 0$ the system is linear and the resulting equations of motion admit an exact solution. [12] developed the solution for a discrete system of resonators, while for a general population, the solution to Eqs. (9) can be solved in closed form. In particular, for a discrete system of resonators $\rho(s) \equiv \rho_N(s)$ as given in Eq. (4) with distribution parameters s_i, $i = 1, \ldots, N$, so that the global self-consistency constants reduce to

$$V = \int_{-\infty}^{\infty} A(n)\rho_N(n)\mathrm{d}n = \frac{1}{N}\sum_{i=1}^{N} A(s_i), \tag{20a}$$

$$W = \int_{-\infty}^{\infty} B(n)\rho_N(n)\mathrm{d}n = \frac{1}{N}\sum_{i=1}^{N} B(s_i). \tag{20b}$$

The distribution of the system of resonators is characterized by the distribution of the values of s_i. In what follows the response of the system is illustrated for a discrete system of resonators, as both the system parameters and number of

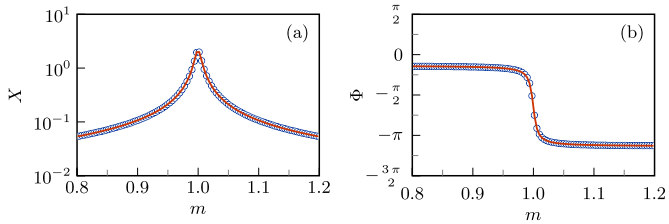

Fig. 1. Linear response functions ($\alpha = 2.00$, $\beta = 5.00$, $\gamma = 0$, $N=100$); —— iterative solution, ◦ ◦ ◦ direct numerical simulation; (a) X, (b) Φ.

elements vary. With a discrete system as given above, defined by the values s_i, the integral equations for $[A(s), B(s)]$ can be solved for any value of s, but only those resonators with $s = s_i$ influence the global self-consistency constants V and W as given in Eqs. (20a).

4.1. Uniform distribution, $N=100$

For illustrative purposes, a uniform distribution of $N=100$ discrete resonators represented by Eq. (4) is chosen with s_i equally spaced within the interval $\epsilon s \in [-0.20, 0.20]$. The amplitude and phase response functions, $X(s)$ and $\Phi(s)$, are shown in Fig. 1 as a function of the resonator mass $m = m_0 + \epsilon s$ with the default parameters of the system. The results of the iterative solution to the amplitude equations given in Eqs. (14b) are represented by the solid line, while the stationary amplitudes obtained from direct numerical simulation of the discrete equations of motion are shown with the marked points. The kernels of the global self-consistency constants (V, W), that is, $A(s)\rho(s)$ and $B(s)\rho(s)$, are shown in Fig. 2 as obtained from the iterative solution. Note that with a uniform distribution these kernels simply reduce to $A(s)$ and $B(s)$, but scaled by the number of oscillators. Consequently, for this distribution, the resonators near $s=0$ ($m = m_0$) contribute most significantly to the global self-consistency constants.

In Figs. 3 and 4 the amplitude and phase response functions are shown for various combinations of α and β. Specifically, in Fig. 3 the response functions are shown for varying α with $\beta = 10.00$; in Fig. 4 the response functions are shown for varying β with $\alpha = 4.00$. As these coupling parameters change the amplitude response functions are primarily scaled by the maximum response. In contrast, for different values of α and β the phase response function is uniformly shifted for all vales of m, indicating that the global coupling introduces an additional phase shift of the resonator population relative to the excitation.

With $\beta = 0$ the global coupling is purely dissipative, and the maximum amplitude is shown in Fig. 5a as the dissipative coupling parameter α is varied. Note that the addition of this global coupling destabilizes the system, and for $\alpha > \alpha_{cr} \approx 12.98$ direct numerical simulation of the equations for the resonator population indicates the system is unstable. In contrast, $\alpha = 0$ corresponds to purely reactive coupling, and the maximum amplitude is shown in Fig. 5b as the reactive coupling parameter β is varied. The addition of such reactive coupling reduces the maximum amplitude of the response.

While the linear system admits an exact solution, for $\gamma \neq 0$ no such closed-form expression exists. However, the amplitude and phase response functions can still be determined with the iterative solution. In Fig. 6 the amplitude and phase response functions for the uniform distribution of resonators are shown for three different values of γ. As expected, $\gamma < 0$ corresponds to a softening response, so that near the resonant frequency the amplitude function is shifted to the left relative to the linear system, while $\gamma > 0$ corresponds to a hardening system. As γ increases the frequency-amplitude shifts become more significant, and can lead to bistability in the system response. Furthermore, as γ varies the maximum amplitude of the response varies as well. This is in contrast to the response of a single resonator with cubic nonlinearity, in which the location in m at which the maximum amplitude occurs shifts, but the value of X_{max} remains constant.

In addition, the response of the system can be considered as the number of discrete resonators varies. In Fig. 7 the response functions are shown for two uniform distributions, one with $N=20$ and the second with $N=1000$. We note that the response of any individual resonator is similar for these two distributions, as the underlying integral equation given in Eq. (14b) depends only on the values of (V, W) defined by Eq. (16). As shown in Fig. 8, as N varies the values of the global self-consistency constants V and W vary significantly for small N, before converging as N increases. The distribution function

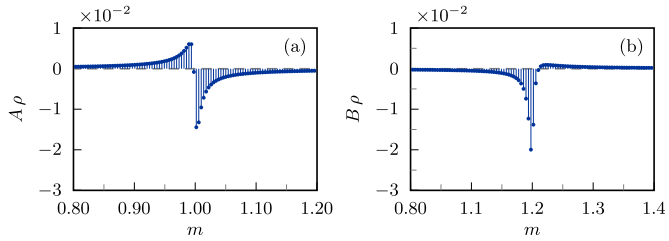

Fig. 2. Coupling kernels ($\alpha = 2.00$, $\beta = 5.00$, $\gamma = 0$, $N=100$, iterative solution); (a) $A\rho$, (b) $B\rho$.

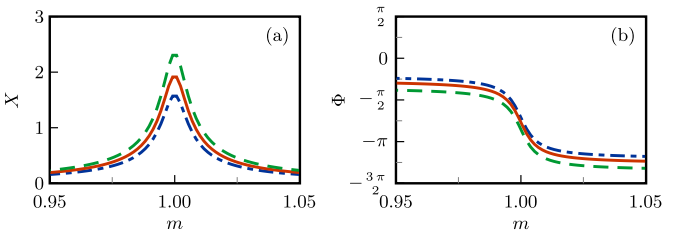

Fig. 3. Linear response functions, varying α ($\beta = 10.00$, $\gamma = 0$, $N = 100$); - - - $\alpha = 0.0$, ——— $\alpha = 4.0$, – – – $\alpha = 8.0$; (a) X, (b) Φ.

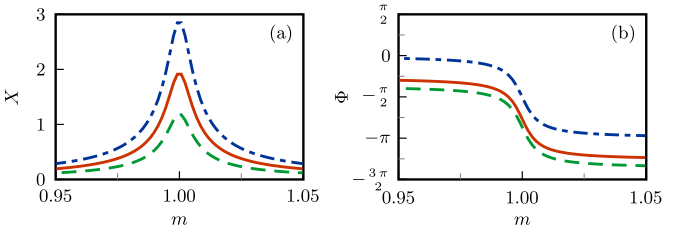

Fig. 4. Linear response functions, varying β ($\alpha = 4.00$, $\gamma = 0$, $N = 100$); - - - $\beta = 0.0$, ——— $\beta = 10.0$, – – – $\beta = 20.0$; (a) X, (b) Φ.

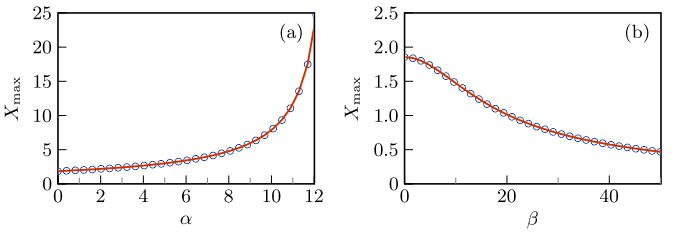

Fig. 5. Maximum response amplitude $X_{\max}$, varying coupling parameters ($\gamma = 0$, $N = 100$); ——— iterative solution, ∘ ∘ ∘ direct numerical simulation; (a) dissipative coupling ($\beta = 0$), (b) reactive coupling ($\alpha = 0$).

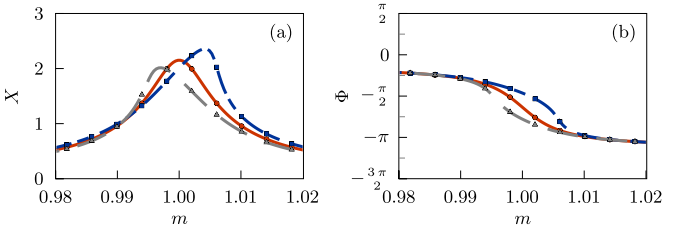

Fig. 6. Nonlinear response functions, varying γ ($\alpha = 2.00$, $\beta = 5.00$, $N = 100$, iterative solutions); -△-△- $\gamma = -0.10$, -○-○- $\gamma = 0$, -■-■- $\gamma = 0.10$; (a) X, (b) Φ.

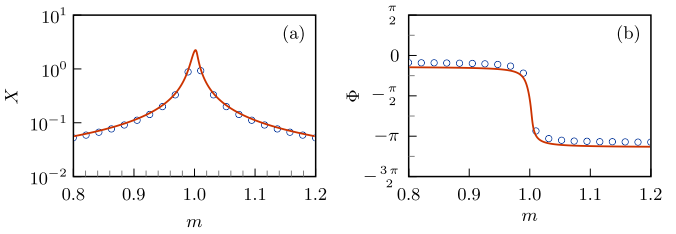

Fig. 7. Response functions ($\alpha = 2.00$, $\beta = 5.00$, $\gamma = 0.05$, iterative solutions); ——— $N = 1000$, ∘ ∘ ∘ $N = 20$; (a) X, (b) Φ.

ρ_N only approaches the uniform distribution as $N \to \infty$. However, as observed in Fig. 8 the global self-consistency constants show little variation above approximately $N = 50$, so that above this population size the discrete population behaves like a continuum distribution. As N increases $(V, W) \to (-0.0286, -0.0824)$ for the parameters utilized herein.

4.2. Other distributions

Perhaps most importantly, the formulation and analytical framework presented herein allow for the consideration of

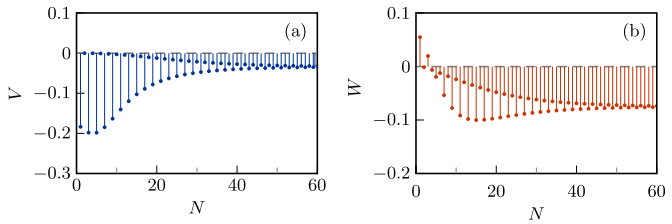

Fig. 8. Global self-consistency constants, varying N ($\alpha = 2.00$, $\beta = 5.00$, $\gamma = 0$, iterative solutions); (a) —— V, (b) —— W.

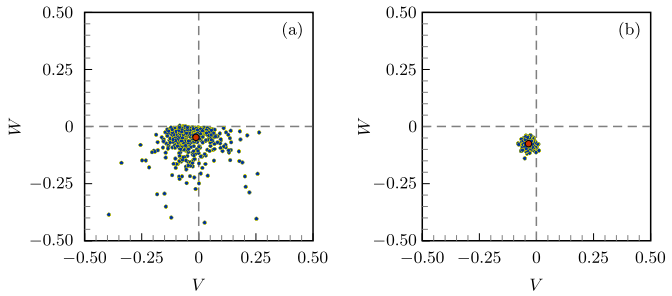

Fig. 9. Global self-consistency constants ($\alpha = 2.00$, $\beta = 5.00$, $\gamma = 0$, iterative solutions, 500 random distributions); (a) $N=20$, (b) $N=500$. The large point indicates the values obtained from the uniform distribution of resonators.

arbitrary distributions of resonators through the population density function $\rho(s)$. As discussed above, the global coupling influences the individual resonators only through the values of V and W, as determined by the self-consistency condition given in Eq. (16). Hence, the iterative approach described above can be applied for any arbitrary resonator distribution.

For the discrete system, the population distribution is defined by the values of s_i defined in Eq. (4). A random distribution of resonators is determined by choosing s_i over the interval $s_i \in [0.80, 1.20]$ with equal probability. Each different distribution results in different values of (V, W), but recall that the values of these global self-consistency constants are determined from the self-consistency condition given in Eq. (16). In Fig. 9, 500 different realizations of the aforementioned distribution are shown for $N=20$ and $N=500$ discrete resonators. The spread in (V, W) is more significant for $N=20$ as compared to $N=500$ indicating that the stationary response is more sensitive to the population distribution for fewer numbers of resonators. For reference the values obtained for the corresponding uniform continuum distribution of resonators are also marked in each figure.

Finally, for a normal distribution of resonators, the global self-consistency constants are shown in Fig. 10 as the standard deviation of the distribution σ varies. Here, the resonator parameters s_i of the discrete distribution are chosen to equally partition the cumulative normal distribution function. Note that in the limit $\sigma \to 0$, each resonator in the population becomes identical and $(V, W) \to (-0.1835, 0.0550)$ for the parameters utilized herein.

5. Conclusions and future work

This work presents a new analytical framework suitable for the analysis of large degree-of-freedom, coupled dynamical systems, which is based upon a four-step process consisting of: (i) a discrete-to-continuous system transformation, with (ii) the application of a perturbation method on the continuum representation, (iii) the use of an iterative numerical method to solve the resulting integral equations, and finally, (iv) the interpretation of the results acquired from the continuous analog or, following an additional transformation, the discrete representation. This methodology should provide utility in the analysis of a wide variety of complex coupled dynamical systems, but is particularly amenable to the design and development of coupled micro- and nanoresonator arrays, such as that explored herein, which commonly exhibit element-level parameter variations, nonlinearity, and/or noise.

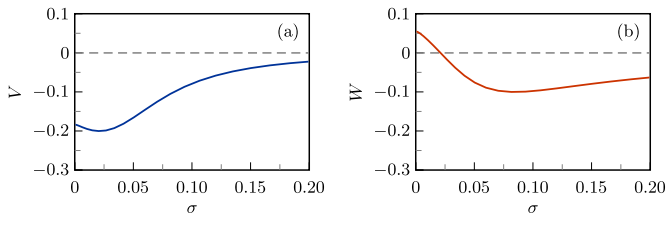

Fig. 10. Global self-consistency constants, iterative solutions, normal distribution varying σ ($\alpha = 2.00$, $\beta = 5.00$, $\gamma = 0$, $N=500$); (a) —— V, (b) —— W.

The analytical framework described in this work is suitable for use with linear and nonlinear systems. However, it is important to note that for $\gamma \neq 0$ the frequency response curves may exhibit bistability, so that for a given s Eq. (14b) admit multiple solutions, and we purposefully avoid such parameter values in this work. When a given system of resonators exhibits bistability, the state of an individual resonator may asymptotically approach a solution on either the upper or lower branch. The global self-consistency constants V and W depend on the asymptotic state of the resonators; thus, to determine these constants one must know the distribution of resonators across the multiple solutions. However, this asymptotic state depends on the initial conditions and transient response of the system, which the perturbation method above cannot address. Therefore, we only consider monostable resonators here, wherein the asymptotic state is unique. The aforementioned research questions surrounding the occurrence of bistability in large degree-of-freedom, coupled dynamical systems, as well as experimental validation of the analytical results presented herein, will be the focus of future work.

Acknowledgements

This material is based upon work supported by the National Science Foundation under Grant Numbers 1537701 and 1537988.

References

[1] T.J. Walker, Acoustic synchrony: two mechanisms in the snowy tree cricket, *Science* 166 (3907) (1969) 891–894.
[2] J. Buck, Synchronous rhythmic flashing of fireflies II, *Q. Rev. Biol.* 63 (3) (1988) 265–289.
[3] M.P. Paidoussis, S. Suss, Stability of a cluster of flexible cylinders in a bounded axial flow, *J. Appl. Mech.* 44 (3) (1977) 401–408.
[4] S.H. Strogatz, From Kuramoto to Crawford: exploring the onset of synchronization in populations of coupled oscillators, *Physica D* 143 (1-4) (2000) 1–20.
[5] C.H. Hodges, Confinement of vibration by structural irregularity, *J. Sound Vib.* 82 (3) (1982) 411–424.
[6] C. Pierre, E.H. Dowell, Localization of vibrations by structural irregularity, *J. Sound Vib.* 114 (3) (1987) 549–564.
[7] J.A. Judge, B.H. Houston, D.M. Photiadis, P.C. Herdic, Effects of disorder in one- and two-dimensional micromechanical resonator arrays for filtering, *J. Sound Vib.* 290 (3–5) (2005) 1119–1140.
[8] A. Erbes, P. Thiruvenkatanathanm, A.A. Seshia, Impact of mode localization on the motional resistance of coupled (MEMS) resonators, in IEEE Frequency Control Symposium (FCS), May 20–24, 2012.
[9] A.B. Sabater, J.F. Rhoads, On the dynamics of two mutually-coupled, electromagnetically-actuated microbeam oscillators, *J. Comput. Nonlinear Dyn.* 7 (3) (2012) 031012.
[10] B.E. DeMartini, J.F. Rhoads, M.A. Zielke, K.G. Owen, S.W. Shaw, K.L. Turner, A single input-single output coupled microresonator array for the detection and identification of multiple analytes, *Appl. Phys. Lett.* 93 (5) (2008) 054102.
[11] J.F. Rhoads, S.W. Shaw, K.L. Turner, Nonlinear dynamics and its applications in micro- and nanoresonators, *J. Dyn. Syst. Meas. Control* 132 (3) (2010) 034001.
[12] A.B. Sabater, J.F. Rhoads, Dynamics of globally and dissipatively coupled resonators, *J. Vib. Acoust.* 137 (2) (2015) 021016.
[13] M. Spletzer, A. Raman, H. Sumali, J.P. Sullivan, Highly sensitive mass detection and identification using vibration localization in coupled microcantilever arrays, *Appl. Phys. Lett.* 92 (11) (2008) 114102.
[14] D.K. Agarwal, J. Woodhouse, A.A. Seshia, Synchronization in a coupled architecture of microelectromechanical oscillators, *J. Appl. Phys.* 115 (16) (2014) 164904.
[15] E. Buks, M.L. Roukes, Electrically tunable collective response in a coupled micromechanical array, *J. Microelectromechanical Syst.* 11 (6) (2002) 802–807.
[16] J. Feng, X. Ye, M. Esashi, T. Ono, Mechanically coupled synchronized resonators for resonant sensing applications, *J. Micromech. Microeng.* 20 (11) (2010) 115001.
[17] R. Lifshitz, M.C. Cross, Response of parametrically driven nonlinear coupled oscillators with application to micromechanical and nanomechanical resonator arrays, *Phys. Rev. B* 67 (13) (2003) 134302.
[18] S. Naik, T. Hikihara, A. Palacios, V. In, H. Vu, P. Longhini, Characterization of synchronization in a unidirectionally coupled system of nonlinear micromechanical resonators, *Sens. Actuators A: Phys.* 171 (2) (2011) 361–369.
[19] S. Naik, T. Hikihara, H. Vu, A. Palacios, V. In, P. Longhini, Local bifurcations of synchronization in self-excited and forced unidirectionally coupled micromechanical resonators, *J. Sound Vib.* 331 (5) (2012) 1127–1142.
[20] M. Sato, B.E. Hubbard, A.J. Sievers, Nonlinear energy localization and its manipulation in micromechanical oscillator arrays, *Rev. Mod. Phys.* 78 (1) (2006) 137–157.
[21] F.C. Hoppensteadt, E.M. Izhikevich, Synchronization of MEMS resonators and mechanical neurocomputing, *IEEE Trans. Circuits Syst. I: Fundam. Theory Appl.* 48 (2) (2001) 133–138.
[22] D.D. Quinn, R.H. Rand, S.H. Strogatz, Singular unlocking transitions in the Winfree model of coupled oscillators, *Phys. Rev. E* 75 (3) (2007) 036218.
[23] A.B. Sabater, A.G. Hunkler, J.F. Rhoads, A single-input, single-output electromagnetically-transduced microresonator array, *J. Micromech. Microeng.* 24 (6) (2014) 065005.
[24] A.B. Sabater, V. Kumar, A. Mahmood, J.F. Rhoads, On the nonlinear dynamics of electromagnetically transduced microresonators, *J. Microelectromech. Syst.* 22 (5) (2013) 1020–1031.
[25] M.V. Requa, K.L. Turner, Electromechanically driven and sensed parametric resonance in silicon microcantilevers, *Appl. Phys. Lett.* 88 (26) (2006) 263508.